Discovery and Characterization of Silver Sulfide Nanoparticles in Final Sewage Sludge Products

BOJEONG KIM,*,† CHEE-SUNG PARK,‡ MITSUHIRO MURAYAMA,‡,§ AND MICHAEL F. HOCHELLA, JR.†,§

The Center for NanoBioEarth, Department of Geosciences, Virginia Tech, Blacksburg, Virginia 24061, Department of Materials Science and Engineering, Virginia Tech, Blacksburg, Virginia 24061, and Institute for Critical Technology and Applied Science, Virginia Tech, Blacksburg, Virginia 24061

Received May 8, 2010. Revised manuscript received August 27, 2010. Accepted September 1, 2010.

Nanosized silver sulfide (α-Ag_2S) particles were identified in the final stage sewage sludge materials of a full-scale municipal wastewater treatment plant using analytical high-resolution transmission electron microscopy. The Ag_2S nanocrystals are in the size range of 5−20 nm with ellipsoidal shape, and they form very small, loosely packed aggregates. Some of the Ag_2S nanoparticles (NPs) have excess S on the surface of the sulfide minerals under S-rich environments, resulting in a ratio of Ag to S close to 1. Considering the current extensive production of Ag NPs and their widespread use in consumer products, it is likely that they are entering wastewater streams and the treatment facilities that process this water. This study suggests that in a reduced, S-rich environment, such as the sedimentation processes during wastewater treatment, nanosized silver sulfides are being formed. This field-scale study provides for the first time nanoparticle-level information of the Ag_2S present in sewage sludge products, and further suggests the role of wastewater treatment processes on transformation of Ag nanoparticles and ionic Ag potentially released from them.

Introduction

The production and use of engineered nanoparticles (NPs) has been increasing dramatically for the past few years. As of 2009, the Project on Emerging Nanotechnologies at the Woodrow Wilson International Center for Scholars had made an inventory of more than 1000 consumer products that claim to have some form of engineered NPs (*1*). Due to the unique antibacterial activity of silver (Ag) (*2*–*5*), Ag NPs are one of the most extensively used NPs in consumer products, and hold great potential for a broad range of future applications. For instance, food storage containers, coating materials, liquid fabric softeners and detergents, fabrics and clothing, sporting goods, dietary supplements, cleaning and personal-care products, cosmetics, and medical appliances that contain Ag NPs are currently available in the marketplace (*6*). Substantial proliferation of Ag nanotechnologies and of uses in consumer products, however, raise environmental concerns over both adverse ecological effects of such particles and Ag ions potentially released from these particles.

To predict the environmental impact of engineered Ag NPs, their characterization from environmental matrices should be pursued, yet no field-scale studies are available to date. In addition, analyses examining the sizes, morphologies, elemental compositions, degrees of crystallinity and atomic structures, coatings, and aggregation states of nanosized Ag particles in the environment are rare (*7*), limiting our ability to conduct a sound risk assessment. Absence of such information may be due to technical difficulties of retrieving trace levels of the Ag NPs from very complex heterogeneous systems. Unlike Ag NPs, there has been some success with identifying nanosized titanium dioxide (TiO_2) in the environment. Specifically, transport of synthetic TiO_2 NPs from exterior facade paints into surface waters was successfully demonstrated in urban areas (*8*). Also, naturally occurring TiO_2 NPs and their strong association with toxic heavy metals have been repeatedly observed in contaminated sediment at the Clark Fork River Superfund Site (*9, 10*).

In a recent risk assessment for engineered Ag NPs, sewage treatment plants are considered to be key intermediate stations that control the most prominent flows of Ag between anthropogenic and environmental compartments (*11, 12*). For example, engineered Ag NPs in consumer products are expected to be released into wastewater streams to a degree during and/or after the lifetime of the products. A recent study demonstrated the ease of extracting Ag NPs and ionic Ag from six commercially available, Ag NP-embedded socks by washing them only with water (*13*). In a separate study, nanosized AgCl particles were identified in the waste solution of a laundry (*14*). At a field scale, however, detailed information regarding Ag NP levels and speciation in wastewater streams, treated plant effluent, and receiving streams from the plant is clearly lacking. During wastewater treatment processes, Ag NPs may be incorporated into the sewage sludge matrix through aggregation and/or sorption reactions and may be concentrated over time. A batch adsorption experiment with Ag NPs and wastewater biomass showed that they would be likely accumulated in the active sewage sludge, in a manner similar to that of ionic Ag (*13*). Therefore, pursuing, identifying, and investigating the nature of Ag NPs in sewage sludge materials is worthy of consideration in order to assess their state when they re-enter the environment through agricultural land application, incineration, or landfilling.

The speciation of Ag NPs collected in settled sewage sludges is also valuable information to wastewater treatment plant managers for operation planning and control. Significant inhibition of bacterial activity by engineered Ag NPs may have an impact on the biological treatment process in the wastewater plant, which in turn impacts the overall performance of the plant. The inhibitory action of engineered Ag NPs on bacterial communities and biofilms has been studied under environmentally relevant conditions (*15*–*17*). The toxicity of Ag NPs will, however, differ once they undergo transformation processes through reacting with environmental constituents. For example, a recent laboratory study demonstrated that the toxicity of Ag NPs on nitrifying bacteria is substantially reduced once they form Ag sulfide complexes/precipitates with sulfide added to the system (*18*).

In January 2009, the United States Environmental Protection Agency (U.S. EPA) released the Targeted National Sewage sludge Survey Statistical (TNSSS) analysis report to evaluate the quality of sewage sludge products generated by the nation's publicly owned treatment works (POTWs) (*19*). The agency collected final sewage sludge samples from 74 POTWs

* Corresponding author phone: 1-540-231-5151; fax: 1-540-231-3386; e-mail: bk74@vt.edu.
† The Center for NanoBioEarth, Department of Geosciences.
‡ Department of Materials Science and Engineering.
§ Institute for Critical Technology and Applied Science.

that are a representative subset of the nation's largest 3337 POTWs. Each POTW is a full-scale municipal wastewater treatment plant, and treats more than one million gallons of wastewater per day, with secondary or better treatment (physical, biological, and/or chemical processes). Data collected from these samples were then extrapolated to cover the entire target population by using appropriate statistical methods (*20*). In this extensive field study, the presence of Ag was identified in all of the sewage sludge samples, and the total concentration of Ag ranged from 1.94 to 856 mg kg^{-1} (on a dry weight basis) (*21*).

The primary objective of this study was to present the first look into the nature of Ag-containing NPs in sewage sludge products collected from a full-scale municipal wastewater treatment plant selected from the U.S. EPA TNSSS analysis report (*19*). The specific aims to achieve the study objective were as follows: (1) to find, positively identify, and characterize the Ag-containing NPs morphologically and chemically by transmission electron microscopy (TEM) and scanning TEM (STEM), combined with energy dispersive X-ray spectroscopy (EDX), (2) to determine the crystal structure of the Ag-containing NPs using high-resolution transmission electron microscopy (HR-TEM) images, and finally, (3) to provide an environmental perspective on the presence of the particular Ag-containing NPs that were found in the final sewage sludge products.

Experimental Section

Sewage Sludge Samples. The U.S. EPA selection criteria for the POTWs and list of toxic pollutants in the final sewage sludge samples were provided in detail in the Sampling and Analysis Technical Report (*20*). In brief, the accompanying TNSSS overview report, described above (*19*), presents concentrations of 28 metals of interest, including Ag, in sewage sludge materials that were sampled from 74 POTWs in 35 states. The sewage sludge samples were sealed in glass jars and kept frozen in an EPA repository (Baltimore, MD) since they were collected. We chose to study the sewage sludge material collected from a POTW located in a metropolitan area of the Midwest region of the U.S. (plant ID no. 27; sample ID no. 68349), because (1) it had the highest Ag content (856 mg kg^{-1}) among the samples tested, and (2) neither photoprocessing plants nor any other identified major industrial user that might discharge massive amounts of Ag are connected to this POTW (U.S. EPA; personal communication). Future studies will include additional samples of interest described in the TNSSS report now that we have refined a sampling and TEM sample preparation protocol (described below) for these samples.

The total S content in this sewage sludge was measured to be 12.0 g kg^{-1} by ICP-AES analysis after employing the EPA-approved, microwave-assisted nitric acid digestion technique in the MARS system (SW 846-3051-Mars, CEM Corp.) (*22*).

Subsamples of the frozen sewage sludge material were taken from the glass jar and were freeze-dried. After freeze-drying, sewage sludge powder samples were gently ground with mortar and pestle. A half-gram of the sewage sludge powder was then added to a 30-mL glass centrifuge tube with 5 mL of deionized water. The sewage sludge slurry solution was mixed thoroughly, and sonicated in a water bath (UltraSonic Bath model 2510, Branson Ultrasonics, maximum frequency at 42 kHz) for one hour. One mL of the slurry solution was diluted 200-fold with methanol (acetone-free, Fisher Scientific), and the concentrations of Ag and S in the methanol extracts were measured by ICP-AES to ensure the presence of these elements in the approximate expected amounts before TEM analysis. This was the case, although the ICP analysis was only semiquantitative due to the methanol (nonaqueous) matrix. A drop of the methanol suspension was placed onto a 200-mesh copper (Cu) TEM grid with lacey carbon support film (Electron Microscopy Sciences, PA), and then allowed to evaporate.

Transmission Electron Microscopy Analyses. Aggregation, morphology, chemistry, and atomic structure of the sewage sludge-born Ag-containing NPs were analyzed by an FEI Titan 80-300 field emission TEM operating at 200 kV. The microscope was equipped with an energy dispersive X-ray (EDX) spectrometer (EDAX r-TEM) for chemical analysis, and a Fischione high angle annular dark field (HAADF) detector was used to sample electrons scattered to relatively high angles (typically about 50−200 mrad) for atomic number (Z)-contrast imaging in the STEM mode. In this study, the chemistry of individual particles of interest was examined with a lateral spatial resolution of approximately 1 nm using the STEM mode. A series of Fast Fourier Transform (FFT) patterns calculated from the HR-TEM images of each NP was used to help identify their crystal structure. FFT patterns calculated from high-resolution, lattice fringe images provide the diffracted electron wave distribution, and are essentially identical to a selected area electron diffraction pattern of the imaged area.

Results and Discussion

Spectroscopic Analysis of Ag-Containing NPs in Sewage Sludge Products. Figure 1a shows a STEM-HAADF image of a representative Ag-containing NP aggregate found in the sewage sludge material. Because the contrast of HAADF images shows Z^2 dependence, particles that contain high atomic number elements (e.g., Ag) are brighter. This particular STEM-HAADF image shows that these Ag NPs found in the sewage sludge material have ellipsoidal shape in the size range of 5−20 nm, and they have formed a very small, loosely packed aggregate.

The EDX spectra of three different Ag NPs (noted as **a**, **b**, and **c**) and an adjacent NP (**d**) are shown in Figure 1b. Spectra for particles **a**, **b**, and **c** always show the presence of sulfur (S). The atomic ratio of Ag to S, calculated from the integrated peak intensity of Ag L and S K lines, is estimated to be 1.7 and 2.1 for particles **a** and **b**, respectively. These semiquantitative values are reasonably close to 2.0 that is expected for the phase Ag_2S. On the other hand, the Ag to S ratio of the particle **c** is about 1.1, displaying a large deviation from that of the other particles. Particle **c** clearly contains excess S relative to Ag_2S, suggesting that Ag sulfidation may be affected by local environments in the sewage sludge. Our finding is in line with a recent laboratory study on the synthesis of Ag_2S NPs through reactions of Ag NPs with H_2S gas (*23*). The majority of the synthetic particles have a Ag to S ratio close to 2 after the reaction, whereas a small fraction possesses a ratio of nearly 1, suggesting the presence of excess S on the surface of the particles (*23*). In addition, S-rich Ag_2S phases (an Ag/S ratio less than 2) have also been identified during the formation of Ag_2S films at the laboratory scale (*24*).

For comparison, we also took the EDX spectrum from NP **d** within the representative NP aggregate shown in Figure 1a. The result of the EDX analysis shows that particle **d** contains no Ag or S, but oxygen (O), silicon (Si), and aluminum (Al). This composition corresponds with the poorer STEM-HAADF image contrast, indicating the absence of heavy elements. Particle **d** is therefore a type of aluminosilicate material in the sewage sludge, the same as many of the particles in this aggregate. Minute particles of these silicates may also be situated underneath or on the top of the very bright Ag-containing NPs, explaining the presence of O, Si, and Al peaks in the EDX spectra of **a**, **b**, and **c**. It is also worth noting that C and Cu peaks appearing in the EDX spectra are most likely from the C support film and/or the surrounding residual sewage sludge organics, as well as the Cu grid sample holder. Often, a hydrogen peroxide-assisted organic oxidation

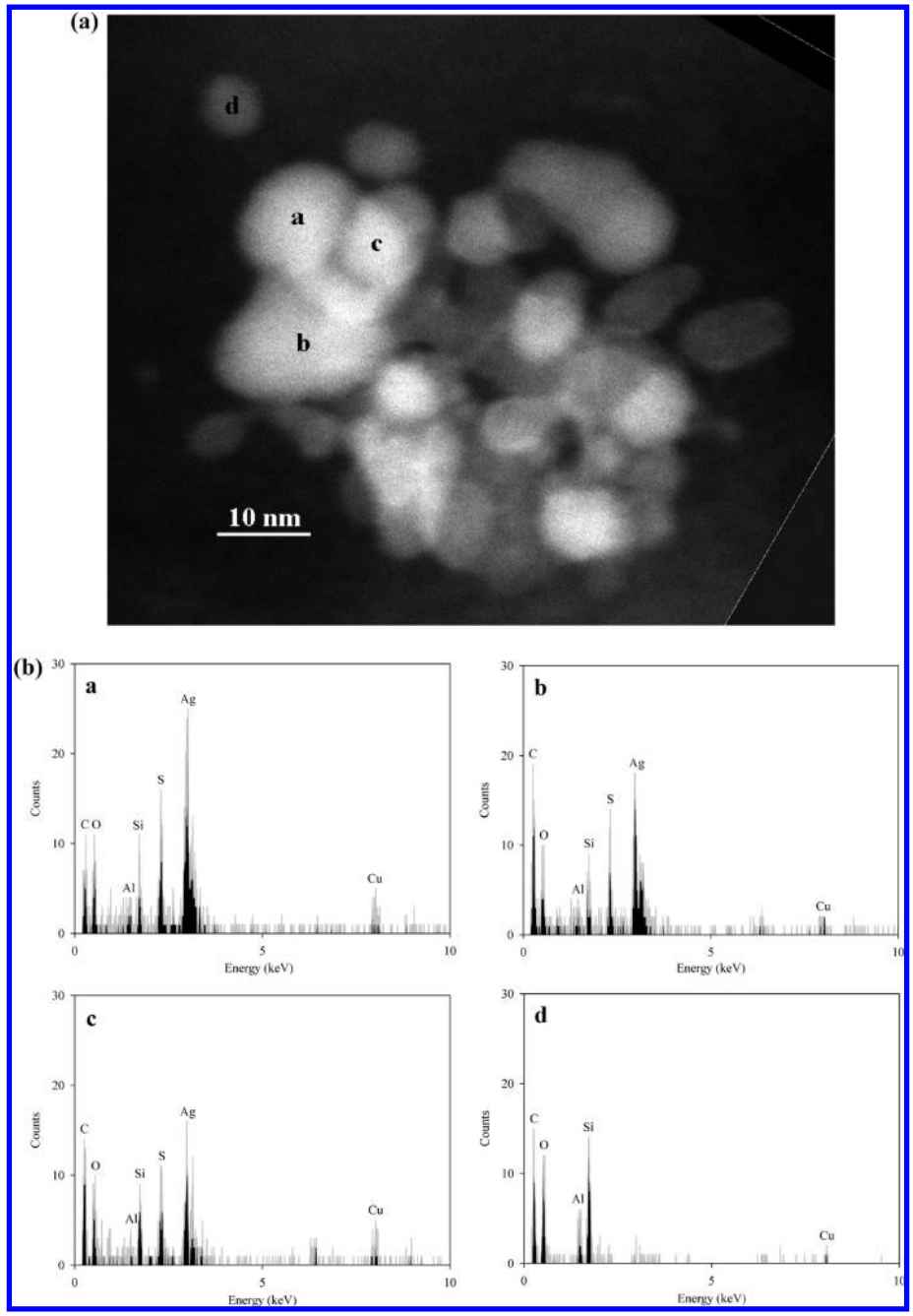

FIGURE 1. Characterization of Ag sulfide nanoparticles in sewage sludge samples: (a) STEM-HAADF image of a representative NP aggregate containing Ag sulfides; (b) energy dispersive X-ray (EDX) spectra of selected particles (a−d) labeled in the image. See text for details.

step is employed for the spectroscopic sample preparation to reduce background interference from high levels of organics in sewage sludge materials (*25*). However, we optimized the sample preparation used here without oxidizing sewage sludge organics, a part of our strategy to preserve the surrounding conditions of the Ag-containing NPs in the matrix.

The STEM-HAADF images of more Ag sulfide NP aggregates found in the sewage sludge material are available in the Supporting Information with the corresponding EDX analyses. These images show that the Ag−S NPs can be as small as 5 nm in diameter.

Structural Analysis of the Ag_2S NPs. To identify the mineral phase of the Ag−S NPs, we have examined the crystal structure of two Ag−S NPs (**a** and **c**) using HR-TEM analysis. Figure 2 shows their HR-TEM image with the inserted TEM bright field image, indicating the position of these particles relative to the STEM-HAADF image (Figure 1). Both particles in the image show two-dimensional lattice fringes, which appear to be essentially identical. This indicates that these two particles were oriented in the same crystallographic direction. The spacing of the most prominent lattice fringes of both particles is 3.48 Å, which is reasonably close to the *d*-spacing of the monoclinic α-Ag_2S (020) plane (3.46 Å) (*26*).

FFT patterns were calculated from the HR-TEM image to more conclusively identify the crystal structure of these Ag sulfide NPs. A FFT pattern of particle **c** (Figure 1 and 2) is provided in Figure 3 with a key diagram. From the *d*-spacing and symmetry of the spot arrangement, the FFT pattern taken from particle **c** was determined to be the monoclinic α-Ag_2S [100] zone axis pattern, i.e., this crystal's [100] direction is parallel to the incident electron beam direction. The key diagram schematically represents the [100] diffraction pattern expected from α-Ag_2S ($a = 4.23$ Å, $b = 6.91$ Å, $c = 7.87$ Å, and

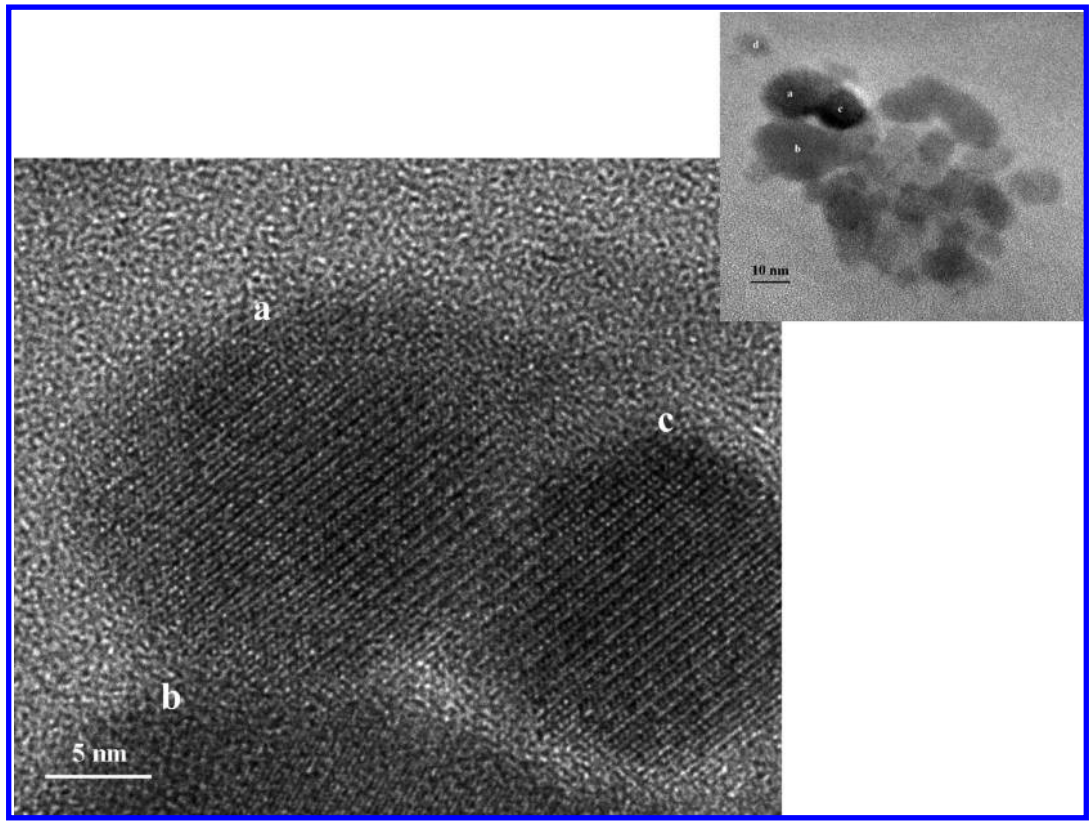

FIGURE 2. HR-TEM image of selected NPs (a and c) in the same orientation as seen in Figure 1. The inset shows a bright-field TEM image of the entire NP aggregate shown in Figure 1.

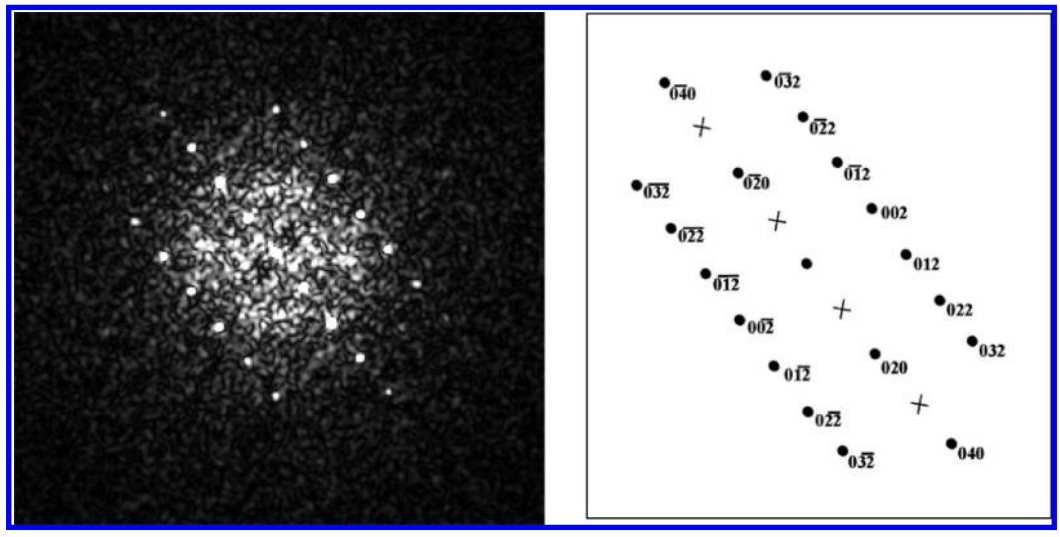

FIGURE 3. An FFT pattern obtained from NP c and a key diagram showing the calculated [1 0 0] pattern for α-Ag_2S. The crosses indicate positions of spots on the FFT pattern that should be systematically absent, but are present due to a defocus of the FFT image.

β = 99° 35′) (*26*). Both diffraction patterns show good agreement except that the FFT pattern has intense {010} spots, which correspond to the strong periodic contrast of every other {020} plane in the original HR-TEM image. According to the symmetry (space group) of this structure, these {010} spots should be absent. However, their presence is caused by a slight defocus of the image, and therefore does not indicate any alteration of the α-Ag_2S structure (*27*).

As previously stated, particle **a** has the ratio of Ag to S of 1.7, whereas particle **c** has a ratio of 1.1. The HR-TEM data and indexing of spots in FFT diffraction patterns confirmed that both particles are α-Ag_2S nanocrystals with the same orientation (Figure 2 and 3). The excess S, therefore, seems not to affect the crystal structure of the particle. Since the α phase of Ag_2S only allows a small degree of compositional deviation (*28*), our finding suggests that Ag_2S nanocrystals are initially formed, but further associated with excess S, resulting in nonstoichiometric relations in the binary system of Ag and S. Presumably, the excess S exists on the surface of Ag_2S minerals by chemisorption.

Anaerobic conditions in the submerged portions of wastewater treatment facilities can be S-rich environments, and formation of Ag_2S in activated sewage sludge systems has been experimentally demonstrated in laboratory studies (*18, 29*). α-Ag_2S is also naturally occurring as the mineral acanthite (*30*). It is polymorphic, and crystallographic transi-

tions of Ag_2S occur at temperatures of 452 and 873 K accompanied with structural changes from monoclinic (α phase) to bcc (β phase) and from bcc (β phase) to fcc (γ phase), respectively (*26*).

Environmental Implication of α-Ag_2S in Sewage Sludge Products. The most likely explanation for our findings is that nanosized α-Ag_2S particles are formed in situ during wastewater treatment by reacting Ag NPs or soluble Ag species with reduced S present under anaerobic conditions. It is very unlikely that the Ag_2S NPs that we observe are naturally occurring acanthite mineral grains, as this is a rare mineral except in certain mining districts. It is not known to be present in metropolitan areas of the Midwestern U.S. On the other hand, at a laboratory scale, chemical transformation of Ag NPs to new Ag_2S or Ag_xS_y species has been demonstrated by adding sulfide to solutions containing Ag NPs (*18*). In earlier studies with photoprocessing discharges, transformation of silver thiosulfate ($Ag(S_2O_3)_n$) complexes to insoluble species (Ag_2S or Ag^0) has been repeatedly shown during wastewater treatment processes (*31*). The type and source of Ag that enter the wastewater plant can vary, but they are likely to form thermodynamically favorable Ag_2S in the presence of reduced S species. Even in sewer systems under anoxic conditions, precipitation of metal sulfide species occurs (*32, 33*). The role of sulfur in metal sequestration via the formation of metal sulfides in aqueous and subsurface systems is well documented (e.g., *34*).

With a detailed understanding of the mineralogy of α-Ag_2S nanocrystals in sewage sludge materials, it is now necessary to investigate the time-dependent changes in their chemical and physical properties when they move into different environments, for example, when sewage sludge material containing Ag_2S NPs is used on agricultural land as soil amendment. Additional processing of sewage sludge materials destined for land application may also have an influence on Ag-containing NP transformation processes. Metal sulfide complexes are, in general, resistant to oxidation and dissociation reactions (*18, 35*). In fact, Ag_2S is known to be one of the most insoluble minerals, with extremely low water solubility (*31*). However, the dissolution rate of galena (PbS) nanocrystals was at least 1 order of magnitude higher than that of galena microcrystals, thus displaying a size-dependent reactivity at the nanoscale (*36*). Sulfide minerals and mineral NPs often play central roles in heavy metal release and mobility over great distances (*37*). Therefore, future studies of size-dependent reactivity, particularly solubility, of Ag_2S NPs will be useful in understanding the environmental fate, influence, and entire life cycle of engineered Ag NPs.

Acknowledgments

This paper was improved by the comments from three anonymous reviewers and the associate editor who handled this publication. We greatly appreciate their efforts. A grant from the National Science Foundation (NSF) and the Environmental Protection Agency (EPA) under NSF Cooperative Agreement EF-0830093, entitled Center for the Environmental Implications of Nanotechnology (CEINT), provided major financial support for this study. Any opinions, findings, conclusions or recommendations expressed in this material are those of the authors and do not necessarily reflect the views of the NSF or the EPA. This work has not been subjected to EPA review and no official endorsement should be inferred. We thank Harry B. McCarty, a senior scientist at the Computer Sciences Corporation and the U.S. EPA for assistance in providing sewage sludge samples for this study. We are appreciative of important assistance from Professor Matthew Eick in the Department of Crop and Soil Environmental Sciences at Virginia Tech, and also from Stephen McCartney and John McIntosh in the Nanoscale Characterization and Fabrication Laboratory at Virginia Tech. B. Kim dedicates this work to Hyoungjin Park, who was always with her for the spectroscopic analyses in the present study, yet could not see this outcome.

Supporting Information Available

STEM-HAADF images and EDX spectra from two more Ag sulfide NP aggregates found in the sewage sludge materials. This material is available free of charge via the Internet at http://pubs.acs.org.

Literature Cited

(1) Woodrow Wilson International Center for Scholars. Nanotechnology Consumer Product Inventory. http://www.nanotechproject.org/inventories/consumer/.

(2) Sondi, I.; Salopek-Sondi, B. Silver nanoparticles as antimicrobial agent: a case study on *E. coli* as a model for gram-negative bacteria. *J. Colloid Interface Sci.* **2004**, *275* (1), 177–182.

(3) Morones, J. R.; Elechiguerra, J. L.; Camacho, A.; Holt, K.; Kouri, J. B.; Ramírez, J. T.; Yacaman, M. J. The bactericidal effect of silver nanoparticles. *Nanotechnology* **2005**, *16* (10), 2346–2353.

(4) Panáček, A.; Kvítek, L.; Prucek, R.; Kolář, M.; Večeřová, R.; Pizúrová, N.; Sharma, V. K.; Nevěčná, T.; Zboěil, R. Silver colloid nanoparticles: Synthesis, characterization, and their antibacterial activity. *J. Phys. Chem. B.* **2006**, *110* (33), 16248–16253.

(5) Baker, C.; Pradhan, A.; Pakstis, L.; Pochan, D. J.; Shah, S. I. Synthesis and antibacterial properties of silver nanoparticles. *J. Nanosci. Nanotechnol.* **2005**, *5* (2), 244–249.

(6) The Project on Emerging Nanotechnologies. Silver nanotechnology: A database of silver nanotechnology in commercial products. http://www.nanotechproject.org/process/assets/files/7039/silver_database_fauss_sept2_final.pdf.

(7) Tiede, K.; Boxall, A. B. A.; Tiede, D.; Tear, S. P.; David, H.; Lewis, J. A robust size-characterisation methodology for studying nanoparticle behaviour in 'real' environmental samples, using hydrodynamic chromatography coupled to ICP-MS. *J. Anal. At. Spectrom.* **2009**, *24* (7), 964–672.

(8) Kaegi, R.; Ulrich, A.; Sinnet, B.; Vonbank, R.; Wichser, A.; Zuleeg, S.; Simmler, H.; Brunner, S.; Vonmont, H.; Burkhardt, M.; Boller, M. Synthetic TiO_2 nanoparticle emission from exterior facades into the aquatic environment. *Environ. Pollut.* **2008**, *156* (2), 233–239.

(9) Plathe, K. L.; von der Kammer, F.; Hassellöv, M.; Moore, J.; Murayama, M.; Hofmann, T.; Hochella, M. F., Jr. Using FIFFF and a TEM to determine trace metal-nanoparticle associations in riverbed sediment. *Environ. Chem.* **2010**, *7* (1), 82–93.

(10) Wigginton, N. S.; Haus, K. L.; Hochella, M. F., Jr. Aquatic environmental nanoparticles. *J. Environ. Monit.* **2007**, *9* (12), 1306–1316.

(11) Gottschalk, F.; Sonderer, T.; Scholz, R. W.; Nowack, B. Modeled environmental concentrations of engineered nanomaterials (TiO_2, ZnO, Ag, CNT, Fullerenes) for different regions. *Environ. Sci. Technol.* **2009**, *43* (24), 9216–9222.

(12) Blaser, S. A.; Scheringer, M.; MacLeod, M.; Hungerbühler, K. Estimation of cumulative aquatic exposure and risk due to silver: Contribution of nano-functionalized plastics and textiles. *Sci. Total Environ.* **2008**, *390* (2−3), 396–409.

(13) Benn, T. M.; Westerhoff, P. Nanoparticle silver release into water from commercially available sock fabrics. *Environ. Sci. Technol.* **2008**, *42* (11), 4133–4139.

(14) Hassellöv, M.; Kaegi, R. Analysis and characterization of manufactured nanoparticles in aquatic environments. In *Environmental and Human Health Impacts of Nanotechnology*; Lead, J. R., Smith, E., Eds.; John Wiley & Sons, Inc.: United Kingdom, 2009; pp 211−266.

(15) Choi, O.; Deng, K. K.; Kim, N.-J.; Ross, L., Jr.; Surampalli, R. Y.; Hu, Z. The inhibitory effects of silver nanoparticles, silver ions, and silver chloride colloids on microbial growth. *Water Res.* **2008**, *42* (12), 3066–3074.

(16) Fabrega, J.; Fawcett, S. R.; Renshaw, J. C.; Lead, J. R. Silver nanoparticle impact on bacterial growth: Effect of pH, concentration, and organic matter. *Environ. Sci. Technol.* **2009**, *43* (19), 7285–7290.

(17) Fabrega, J.; Renshaw, J. C.; Lead, J. R. Interactions of silver nanoparticles with *Pseudomonas putida* biofilms. *Environ. Sci. Technol.* **2009**, *43* (23), 9004–9009.

(18) Choi, O.; Clevenger, T. E.; Deng, B.; Surampalli, R. Y.; Ross, L., Jr.; Hu, Z. Role of sulfide and ligand strength in controlling nanosilver toxicity. *Water Res.* **2009**, *43* (7), 1879–1886.
(19) USEPA. Targeted National Sewage sludge Survey Statistical Analysis Report. http://epa.gov/waterscience/biosolids/tnsss-stat.pdf.
(20) USEPA. Targeted National Sewage sludge Survey Sampling and Analysis Technical Report. http://water.epa.gov/scitech/wastetech/biosolids/upload/2009_01_15_biosolids_tnsss-tech.pdf.
(21) USEPA. Targeted National Sewage sludge Survey Statistical Analysis Report (Appendix A). http://water.epa.gov/scitech/wastetech/biosolids/upload/appendixa.pdf.
(22) CEM Corporation. Application notes (analytical). http://www.cem.com/index.php.
(23) Chen, R.; Nuhfer, N. T.; Moussa, L.; Moprris, H. R.; Whitmore, P. M. Silver sulfide nanoparticle assembly obtained by reacting an assembled silver nanoparticle template with hydrogen sulfide gas. *Nanotechnology* **2008**, *19* (45), 1–11.
(24) Kundu, M.; Terabe, K.; Hasegawa, T.; Aono, M. Effect of sulfurization conditions and post-deposition annealing treatment of structural and electrical properties of silver sulfide films. *J. Appl. Phys.* **2006**, *99* (10), 103501.
(25) Kiser, M. A.; Westerhoff, P.; Benn, T.; Wang, Y.; Pérez-Rivera, J.; Hristovski, K. Titanium nanomaterial removal and release from wastewater treatment plants. *Environ. Sci. Technol.* **2009**, *43* (17), 6757–6763.
(26) Frueh, A. J., Jr. The crystallography of silver sulfide, Ag_2S. *Z. Kristallogr.* **1958**, *110*, 136–144.
(27) Fultz, B.; Howe, J. *Transmission Electron Microscopy and Diffractometry of Materials*; Springer: New York, 2001; pp 523−593.
(28) Kracek, F. C. Phase relations in the system sulfur-silver and the transitions in silver sulfide. *Trans. Am. Geophys. Union* **1946**, *27*, 364–374.
(29) Pavlostathis, S. G.; Maeng, S. K. Fate and effect of silver on the anaerobic digestion process. *Water Res.* **2000**, *34* (16), 3957–3966.
(30) Purcell, T. W.; Peters, J. J. Sources of silver in the environment. *Environ. Toxicol. Chem.* **1998**, *17* (4), 539–546.
(31) Lytle, P. E. Fate and speciation of silver in publicly owned treatment works. *Environ. Toxicol. Chem.* **1984**, *3* (1), 21−30.
(32) Houhou, J.; Lartiges, B. S.; Montarges-Pelletier, E.; Sieliechi, J.; Ghanbaja, J.; Kohler, A. Sources, nature, and fate of heavy metal-bearing particles in the sewer system. *Sci. Total Environ.* **2009**, *407* (23), 6052–6062.
(33) El Samrani, A. G.; Lartiges, B. S.; Ghanbaja, J.; Yvon, J.; Kohler, A. Trace element carriers in combined sewer during dry and wet weather: an electron microscope investigation. *Water Res.* **2004**, *38* (8), 2063–2076.
(34) Rickard, D.; Luther , G. W., III Metal sulfide complexes and clusters. In *Reviews in Mineralogy & Geochemistry*; Vaughan, D. J., Ed.; Mineralogical Society of America: Washington, DC, 2006; Vol. 61, pp 421−504.
(35) Rozan, T. F.; Lassman, M. E.; Ridge, D. P.; Luther, G. W., III. Evidence for iron, copper and zinc complexation as multinuclear sulphide clusters in oxic rivers. *Nature* **2000**, *406* (6798), 879–882.
(36) Liu, J.; Aruguete, D. M.; Murayama, M.; Hochella, M. F., Jr. Influence of size and aggregation on the reactivity of an environmental and industrially relevant nanomaterial (PbS). *Environ. Sci. Technol.* **2009**, *43* (21), 8178–8183.
(37) Hochella, M. F., Jr.; Moore, J. N.; Putnis, C.; Putnis, A.; Kasama, T.; Eberl, D. D. Direct observation of heavy metal-mineral association from the Clark Fork River Superfund Complex: Implications for metal transport and bioavailability. *Geochim. Cosmochim. Acta* **2005**, *69* (7), 1651–1663.

ES101565J